Optical Position Sensor Based on Digital Image Processing: Magnetic Field Mapping Improvement

Ondrej PRIBULA, Michal JANOŠEK, Jan FISCHER

Dept. of Measurement, Czech Technical University in Prague, Faculty of Electrical Engineering, Technická 2, 166 27 Prague, Czech Republic

ondrej.pribula@fel.cvut.cz, michal.janosek@fel.cvut.cz, fischer@fel.cvut.cz

Abstract. *Optical position measurement system for an automated magnetic field mapping apparatus based on fluxgate sensors is presented. For the exact position estimation of the sensor head, a simple smart camera was developed with respect to minimal hardware configuration and real-time execution of position measurement algorithm. The camera is observing the mapped scene and evaluates position of the sensor head using an active marker. The sensor head is designed as movable, what allows keeping the scene fixed and exactly referenced to the mapped magnetic field using coordinates obtained from image. With image sensor fixed 2.5 m above the plane and range ±130 mm around the lens optical axis (image center), the total position measurement error is less than 0.5 mm.*

Keywords

Position measurement, smart camera, magnetic field mapping.

1. Introduction

In the field of magnetic measurements one of frequent tasks is to measure magnetic field distribution – magnetic field mapping. Field mapping is used for example for ferromagnetic markers detection in biomedical diagnostics. One of possible methods for mapping of magnetic field is to use a movable sensor head which is moved along the scanned area [1]. Position of the head and measured value are processed to obtain a 2D magnetic field map.

A crucial task that influences the overall mapping spatial resolution is position estimation of the moving head. If DC magnetic fields in order of 10^{-9} T are to be measured, it is necessary to ensure that the measured magnetic field is not affected by the measurement method or the used instrument (by construction parts of the position sensor). Thus the position measurement has to be based on a contactless method that allows the position sensor to be placed in an adequate distance not affecting the measured field by its construction parts (e.g. metal components). A reasonable solution is to use an optical principle for position measurement, which allows using even non-perfect positioning stage with a non-magnetic sensor arm, avoiding the need for expensive, non-magnetic positioning systems, which are also limited in service-life.

For high precision position measurement a laser-interferometer can be used. Spatial resolution of a multi-dimensional position measurement system [2] is about 0.07 mm in wide-range, but construction severity and price are very high. For the task of magnetic field mapping, about 1 mm spatial resolution of the measurement head position is satisfactory (in the range of 700mm x 700 mm). Thus position measurement based on digital image processing is reasonable allowing for lower complexity and costs.

With the growing performance of computational tools, image-based measurement systems are frequently used instead of conventional sensors (sets of sensors) for measurements of physical quantities (measured quantity has to be convertible to visually observable form). Generally image-based sensors can be constructed as *PC-based Systems* (image information is acquired by an external camera connected to a PC using a frame-grabber, image is processed in the PC), *Stand-alone Image Processing Units* (external camera is connected to a stand-alone processing unit whose performance is optimized for image processing algorithms) or *Smart Cameras* (devices which are embedding image acquisition and processing into a single device). The basic advantage of the last mentioned sensors is their compactness and portability, providing still adequate computational performance for less demanding algorithms.

Complexity of the algorithm can be decreased using a-priori information that simplifies image processing. For the position measurement task such simplification can be a well-defined object (marker), fixed to the object whose position is evaluated. If this object has significant and unique brightness profile it is very simple to recognize it in the observed scene and calculate its position. For the real world measurements objects of interest are usually not easy recognizable, but in many tasks an external marker can be added to highlight the measured object. This approach when extra information is added into the image of the measured object to simplify the image processing is called *Assisted Videometry*.

In our case of the magnetic field mapping apparatus a Light Emitting Diode (LED) is fixed on the movable sensor head and serves as an active marker simplifying image processing. Less demands on image-processing performance allowed us to choose a smart camera variant as appropriate for our purpose, adding portability of the position sensor.

The developed smart camera for position measurement utilizes a complementary metal oxide semiconductor (CMOS) image sensor [3] as the image information source. Computational and control core is based on the digital signal processor (DSP) Blackfin® (Analog Devices, Inc.). A set of standard communication peripherals (USB, RS-485, RS-232 etc.) was implemented to simplify connecting into a measurement chain.

Utilizing the smart camera as coordinates referencing system allows easy mapping of the measured magnetic field into the acquired image of the measured scene. Particularly in medical applications, when scanned ferromagnetic particles are forming a marker, the result (mapped field) could be directly referenced to the camera image of the affected part of the human body. This visualization method – image mapped magnetic field can simplify the medical pre-treatment decision process [4].

The following paragraphs of this paper cover construction of a simple smart camera based on CMOS image sensor and DSP, the optical front-end and its relation with position measurement results, image processing algorithm used for position estimation and finally discuss the position measurement results with the main focus on achieved precision. A novel apparatus for magnetic field mapping based on the flux-gate sensors and the developed position sensor is introduced together with magnetic field mapping results.

2. Smart Camera as a Position Sensor

Optical referencing of the sensor arm position is solved by use of a simple smart camera designed for an embedded implementation of image processing algorithms (contact-less optical measurement evaluation).

As a computational core of the smart camera usually the Field Programmable Gate Array (FPGA), digital signal processor or combination of both technologies can be used. Solutions based on the FPGA may have a high image processing performance, but reconfiguration of those systems is a time-consuming task [5]. The published DSP-based smart camera conceptions are usually equipped with a slow communication interface with the PC (comfortless due to the slow transfer rate of image data to the PC) or are lacking hardware synchronization of the measurement, which is important for data post-processing [6].

The real-time position measurement, with a-priori information in form of a marker (a point light source - LED) was implemented in a minimalistic concept of a simple smart camera based on DSP as introduced below.

2.1 DSP-Based Smart Camera Conception

Considering the mentioned real-time performance requirements and image source of CMOS technology with the direct digital interface, ADSP-BF532 Blackfin® digital signal processor was selected as a reasonable solution core. Blackfin® processor is equipped with the integrated Parallel Peripheral Interface (PPI) that in cooperation with the dedicated Direct Memory Access (DMA) channel provides a glue-less interface to the CMOS image sensor. Using this feature, almost all processor time can be effectively used for image processing (processor doesn't need to control transfer of image data from the image sensor, it is done in the background).

The hardware of the smart camera is equipped with an additional 1 MB of data SRAM and a USB Full Speed driver chip for communication with PC. For synchronization of measurements a set of optically isolated inputs and outputs is available. Interface to the measurement chain is also provided by a RS-485 interface. The smart camera block diagram is depicted in Fig. 1.

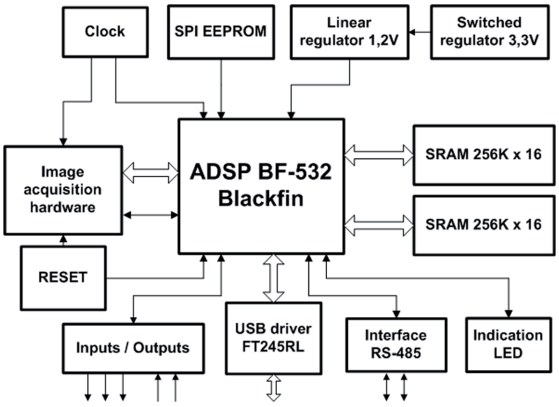

Fig. 1. The designed smart camera block diagram

CMOS image sensor LM9638 was used for image acquisition. Physical resolution of this image sensor is 1312x1032 pixels. Effective resolution of this image sensor is 1288 x 1032 pixels (the difference between the full physical resolution and the effective resolution is given by a group of shadowed pixels that are used for sensor calibration and image corrections). For the purpose of our measurement where the position resolution about 1 mm was required, we used a window of standard resolution of 1280x1024 pixels, which was reduced to 640x512 pixels by down-sampling using an on-chip 2x2 pixel-averaging function (binning). Decreasing of the image resolution proportionally reduced also the execution time of implemented algorithms (described below). Physical dimensions of the active photosensitive area are 7.68 x 6.144 mm with the virtual pixel size (after down sampling) 12 μm (square pixel).

2.2 Smart Camera Optical Front-End

The smart camera was equipped with a lens with fixed focal length of 25 mm (Carl Zeiss, Tevidon 1.8/25).

Lens quality is strongly affecting the final measurement nonlinearity due to geometrical errors which are distorting the acquired image. A color filter was mounted on the lens for highlighting of the optical marker and suppressing the background scene (the marker and the filter were of the same color).

Optical front-end and marker projection on the image sensor is depicted in Fig. 2. Equation (1) describes the relationship between the horizontal field of view V_H and distance d between the measured plane and the camera lens principal point. In this equation f stands for the lens focal length and S_H denotes the horizontal size of the photosensitive area of the image sensor. The relation is calculated for a 25 mm lens and the image sensor with above the described parameters.

$$V_H = \frac{d-f}{f}\cdot S_H = \frac{d-25\cdot10^{-3}}{25\cdot10^{-3}}\cdot 7.68\cdot10^{-3}\ \ [m,m] \quad (1)$$

By exchange of parameter S_H with S_V (vertical size of the photosensitive area) equation (1) calculates vertical field of view V_V of the smart camera. View area can be also represented by the diagonal angle of view

$$\omega = 2\cdot arctg\left(\frac{\sqrt{S_H{}^2+S_V{}^2}}{2.\left(f+\frac{f^2}{d-f}\right)}\right). \quad (2)$$

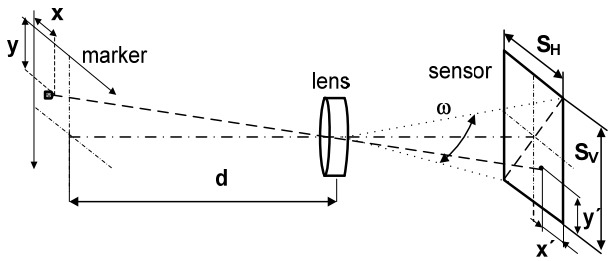

Fig. 2. Smart camera optical front-end and marker projection (distances are not depicted in real ratios).

Position of the object projected on the image sensor is evaluated in pixels. For calculation into real-world units equation (3) is used

$$k = \frac{f}{(d-f).S_P} = \frac{25.10^{-3}}{(d-25.10^{-3}).12.10^{-6}} \quad [pixel/m]. \quad (3)$$

In (3) k stands for calibration constant (pixel/m) and S_P denotes pixel size.

2.3 Image Processing Algorithm

The principle of position estimation is based on the evaluation of active marker position – its brightness profile is depicted in Fig. 3. However the LED supply current is a source of an additional magnetic field that can interact with the mapped field and thus increase magnetic field measurement error. Therefore the LED is controlled by smart camera output and it is activated only during the time of image acquisition which is different from acquisition of the magnetic data.

Another possible solution would be an optical fiber, or a retro-reflexive material with an external light source could be used on the position of the active marker (in both cases the real light or illumination source must be placed in the distance where it is not affecting the measured magnetic field).

The estimated position of the active marker is calculated as a position of the group of image pixels with the highest intensities.

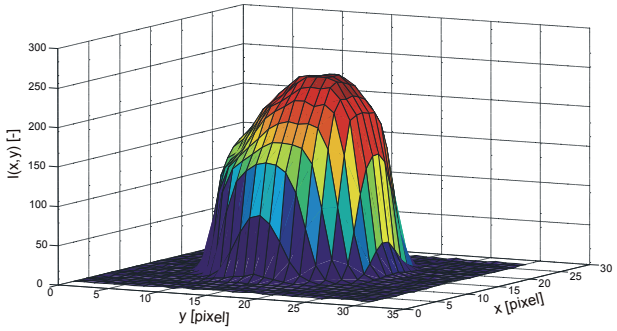

Fig. 3. Spatial profile of LED brightness (lens aperture set to avoid image saturation).

Assuming only one marker, significantly brighter than its background, a center of image gravity formula derived from a 2D object barycenter calculation can be used for its position estimation [7]. Its discretized form for grayscale image (4) is proper for real-time implementation with digital signal processor

$$T_X = \frac{\sum_{y=0}^{H-1}\sum_{x=0}^{W-1} xI(x,y)}{\sum_{y=0}^{H-1}\sum_{x=0}^{W-1} I(x,y)},\ T_y = \frac{\sum_{y=0}^{H-1}\sum_{x=0}^{W-1} yI(x,y)}{\sum_{y=0}^{H-1}\sum_{x=0}^{W-1} I(x,y)}. \quad (4)$$

In the previous equation T_x and T_y denote coordinates of the gravity center, $I(x,y)$ stands for image intensity value at the given point, x and y represent current coordinates in the processed image of width W and height H (in pixels).

To ensure that only the pixels of the light source will be used in the calculation and the rest of the acquired image will be suppressed, the image is preprocessed using a grayscale threshold function. Pixels with intensities below the selected level are suppressed (their intensity value is calculated as 0) [8].

Due to the integral character of the calculation, resolution of obtained results is always higher than the smallest picture element (sub-pixel resolution). This feature is advantageous as no additional input data interpolation is needed and calculation provides sub-pixel results by itself. Position measurement dynamics increases abreast with the constant computation performance (for higher precision of measurement result no additional processor time is needed).

The average time needed for single image (frame) processing and position calculation, with a 5 mm marker presented in the scene and with the use of the algorithm described above, was approximately 23 ms (digital signal processor core running on 400 MHz).

2.4 Position Measurement Precision

The algorithm for position estimation according to (3) was discussed in [9], where its precision is measured with artificial data set: the application of threshold and noise in image data are identified as general error sources. However in the real measurement also the error caused by geometrical errors of the lens has to be considered as a source of position measurement nonlinearity.

Real-world precision of position measurement was investigated using a linear positioning stage with a step of 50 µm (position was measured by linear incremental optical sensor with resolution of 5µm). The LED marker was fixed on the stage and arranged in the middle part of the view area and moved horizontally (along the image sensor line).

For the reduced measurement range of 260 mm (centered to the optical center of the lens) and the camera distance d of 2.5m (V_H = 760 mm) above the measured plane the calibration coefficient k (3) was 847.75 pixel/m (1 pixel = 1.18 mm).

Although the sensor was not totally perpendicular to the measured plane very good results in terms of resolution and linearity were obtained. The total position measurement error was lower than 0.48 mm which causes linearity error about 0.18 % of full–scale (260 mm), see Fig. 4. In the area very close to the optical center (± 30 mm at 120 mm in Fig. 4), where the geometrical error caused by optics is minimal, the total error was less than 0.1% of the full-scale. The position fluctuations (visible in Fig. 4) are primarily caused by noise contained in the input image information.

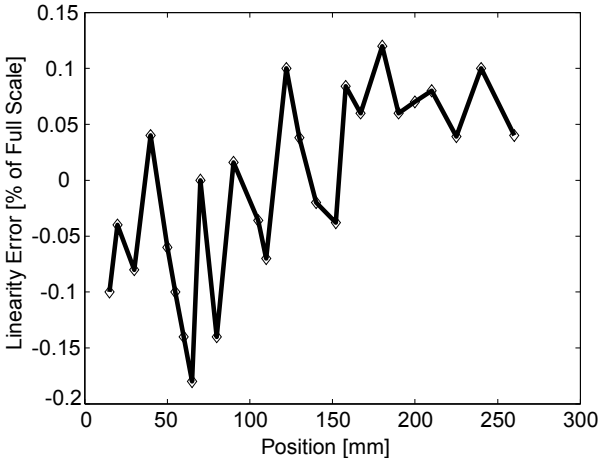

Fig. 4. Relative linearity error of the position measurement results (full-scale horizontal range).

Time-fluctuation of the measured position value (in pixels) with fixed LED marker position is depicted in Fig. 5. Other possible source of nonlinearity in evaluated results can be mechanical construction of the used linear positioning stage with its position uncertainty.

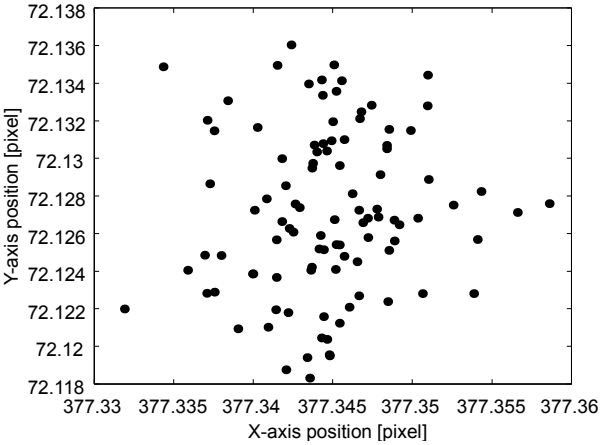

Fig. 5. Fluctuation of the measured position in set of 100 measurements (LED marker position is fixed).

If higher resolution than 1mm, which is satisfactory in the magnetic field mapping task, is required, an averaging function could be applied to the measured set of positions and position resolution could be thus increased.

3. Magnetic Field Mapping System Setup

The motivation for the development of the smart-camera based positioning system was an improvement of the existing magnetic field-mapping system. Generally, there are two concepts of automated positioning when mapping magnetic fields – holding the sensor (array) fixed and moving the scene, or vice versa. The first option is more robust and does not suffer from non-homogeneity of the background magnetic field, however, it is limited in the size of the moved object. This approach was used in mapping of the field gradient in magnetopneumography [4], where moving of the whole human body on a non-magnetic bed makes the measurement time-consuming and inefficient.

However a movable sensor head offers more flexibility and is popular in commercial solutions, as moving the sensor head is usually less complex and allows easy fitting to the measured object [1]. Because the magnetic cleanliness of commercially positioning systems is often questionable we used our positioning device made from a rebuilt XY-recorder, with steel parts removed and replaced, in order to keep intrinsic magnetic moment to minimum. The movable sensor head was placed on an 80 cm long non-magnetic arm and allowed a 40 x 40 cm scene to be positioned on. On the sensor arm, a LED diode (as an active marker) was placed near the sensor head, forming the

reference point to the coordinates as obtained from the smart-camera. The 5 mm shift between the marker and the center of the fluxgate sensors was numerically corrected in all the measurements. The developed position sensor was mounted 2.5 m above the measured object (Fig. 6).

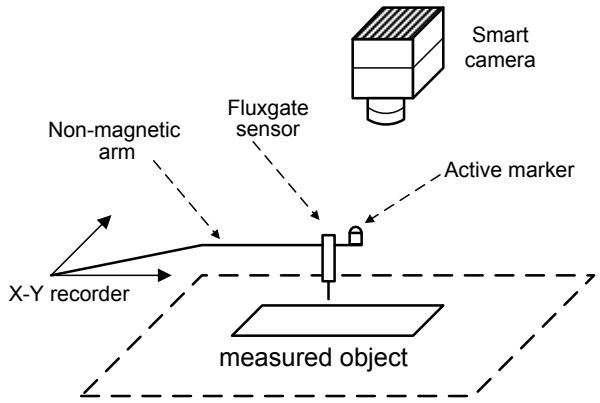

Fig. 6. Magnetic field mapping system setup.

As a magnetic field sensor, flat printed-circuit-board (PCB) fluxgate sensors of our own design were used, as they can be easily fixed in orthogonal or gradiometric setup and are sensitive enough to detect magnetic fields in nT range [10]. The sensor dimensions are 33.5 x 15.5 x 0.9 mm^3, the low thickness allowed to mount the sensors forming a first order dBx/dy gradiometer with very small gradiometric base (1 mm were used) sensor distance.

The sensors were operated in the 2nd harmonic mode, without any feedback loop, and the output voltage from the lock-in amplifier SR-830 (either in A or A-B mode in gradiometric setup) was fed to the acquisition system consisting of 2 HP 34401 multimeters in 6.5 digits resolution.

Together with a programmable DC-current source, which generated voltages for X and Y inputs of the XY-recorder, the setup was automatically driven with LabView software which was linked to the smart-camera based position sensor with a USB interface providing coordinates reference for the positioning and data-acquisition.

3.1 Improved Magnetic Filed Mapping - Results

For evaluation of the designed setup, we visualized the remanent magnetic field of a PCB board, containing magnetometer's analog electronics used on the Czech scientific satellite Mimosa [10].

As the board was placed perpendicular to the normal component of Earth's field, which is almost 80% in our region, we could map the influence of magnetically hard and soft components magnetized by that field. We placed the sensor arm 15 mm above the PCB, the mapped normal component (after subtracting the offset due to Earth's magnetic field) is shown in Fig. 7 – 1V corresponds to approx. 0.5 µT, which is 1/10 of Earth's field value and can be already in the level of environmental noise. The usability of the smart camera position sensor is not only in the overlay of measured data and the scene, but it also ensures orthogonal grid, either by the used feedback-loop, where the positioning device is referenced to the camera position readings, or by the means of post-processing in Matlab.

As the measured area was still affected by the local magnetic field inhomogeneity, we decided to use the gradiometric setup as described above, with the result shown in Fig. 7. The measurement step was refined to 2 mm and we were able to clearly identify a magnetic screw in the D-SUB connector, a foil capacitor and an EEPROM as main magnetically disturbing parts.

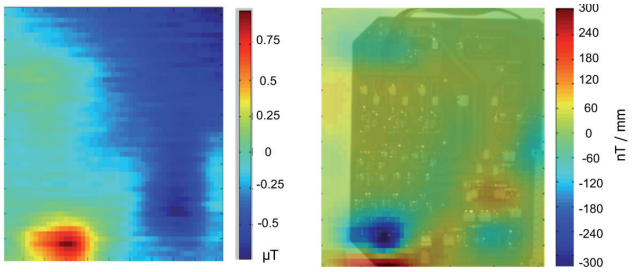

Fig. 7. Mapped normal field (left) and gradient (right) distribution 15mm above the plane.

With the help of gradiometric reading, we succeeded in mapping of the remanent field of a 1-USD banknote at 5 mm height, without any external field excitation (early results were presented in [11] but did not allow to map the data precisely without the use of position sensor). The obtained image could be transformed and fitted to the camera image, resulting in Fig. 8. The depicted magnetic gradient is less than 20 nT/mm and thus the system with a contactless smart-camera based optical position sensor has proven feasible for sensitive DC magnetic field mapping in real unshielded environment.

Fig. 8. Mapped gradient field of a 1-USD banknote, as measured 5 mm above the plane.

4. Conclusion

We have developed an optical position measurement sensor based on image information processing. The sensor was designed as the stand-alone device based on digital signal processor Blackfin® and CMOS image sensor. Basic motivation for the sensor development was improvement of a method for 2D magnetic field mapping by increasing its spatial resolution.

Although the required and fully satisfactory position resolution was about 1 mm, the total position measurement error of the developed sensor was less than 0.5 mm which results non-linearity about 0.2 % of the full–scale. In the area very close to the optical center (± 30 mm) this non-linearity was less than 0.1%. Position measurement uncertainty can be decreased by averaging of measured values.

With the use of the developed camera as a position sensor for the magnetic field mapping system, the measured magnetic field distribution can be directly mapped into the acquired image of the mapped object and thus improve results interpretation (e.g. for field mapping in medicine).

Acknowledgements

Research described was supported by research program No. MSM6840770015, sponsored by the Ministry of Education, Youth and Sports of the Czech Republic and by the Czech Agency Grant No. GA 102/09/H082.

References

[1] TUMANSKI, S., LISZKA, A. The methods and devices for scanning of magnetic fields. *Journal of Magnetic Materials*, 2002, vol. 242-245, Part 2, p. 1253-1256.

[2] YONGBING, L., GUOXIONG, Z. The optimal arrangement of four laser tracking interferometers in 3D coordinate measuring system based on multi-lateration. In *IEEE International Symposium on Virtual Environments, Human-Computer Interfaces and Measurement Systems 2003. VECIMS '03.* 2003, p. 138- 143, doi: 10.1109/VECIMS.2003.1227044.

[3] El GAMAL, A., ELTOUKHY, H. CMOS image sensors. *IEEE Circuits and Devices Magazine*, May-June 2005, vol. 21, no. 3, p. 6- 20, doi:10.1109/MCD.2005.1438751

[4] TOMEK, J., PLATIL, A., RIPKA, P., KASPAR, P. Application of fluxgate gradiometer in magnetopneumography. *Sensors and Actuators A: Physical,* 2006, vol. 132, no 1, p. 214-217.

[5] LEESER, M., MILLER, S., YU, H. Smart camera based on reconfigurable hardware enables diverse real-time applications. In Proceedings of the *12th Annual IEEE Symposium on Field-Programmable Custom Computing Machines*, 2004. IEEE Computer Society, Washington DC, p. 147-155.

[6] LOVVEL-SMITH, C. D., BONES, J. P., HAYES, M. P., JOHNSTON, R.A., PRICE, N. B. 'Black Spot': A prototype camera module. In *Proceedings of the 23rd International Conference on Image and Vision Computing.* New Zealand, 2008, p.1-6, doi: 10.1109/IVCNZ.2008.4762112M

[7] SHORTIS, R., CLARKE, T. A., SHORT, T. A comparison of some techniques for the subpixel location of discrete target images. *Videometrics III,* SPIE vol. 2350. Boston. p. 239-250.

[8] FISCHER, J., ODLOZIL, P. FPGA based system for the measurement of a laser spot position. In *Proceedings of Eurosensors XVI*. Prague, 2002, p. 201-202, ISBN 80-01-02576-4

[9] EGMONTON-PETERSEN, M., REIBER, J. H. C. Accurate object localization in gray level images using the center of gravity measure: Accuracy versus precision. *IEEE Transactions on Image Processing,* 2002, vol 11, no. 12, p 1379 - 1384, doi: 10.1109/TIP.2002.806250

[10] JANOSEK, M., RIPKA, P. PCB sensors in fluxgate magnetometer with controlled excitation. *Sensors and Actuators A: Physical,* April 2009, vol. 151, no. 2, p. 141-144, ISSN 0924-4247, doi: 10.1016/j.sna.2009.02.002

[11] JANOSEK, M., RIPKA, P., PLATIL, A. Magnetic markers detection using PCB fluxgate array. *Journal of Applied Physics*, 2009, vol. 105, no. 7, p. 7E717. ISSN 0021-8979

About Authors ...

Ondrej PRIBULA received his M.Sc. at the Faculty of Electrical Engineering (FEE), Czech Technical University in Prague (CTU) in 2007. At present he is pursuing the Ph.D. at CTU, FEE, Department of Measurement. His main research interests are in the field of precise optical measurement based on smart cameras, CMOS sensors with embedded image processing with DSP and FPGA.

Michal JANOŠEK graduated from the FEE, CTU in 2007 (Dept. of Measurement - Measurement and Instrumentation) and is now pursuing the PhD degree at the same department. His main research activity is the application of magnetic sensors in sensing and detection of ferromagnetic objects and development in PCB fluxgate sensors.

Jan FISCHER received his M.Sc. and Ph.D. degrees in Electrical Engineering from the FEE, CTU, in 1977 and 1989, respectively. He is an Assistant Professor with the Department of Measurement, FEE, CTU. His current research topics include development of methods for image based measurement and application of CCD sensors and DSP in measuring instruments.